# COMMANDER results on PICO (PSM)

Mathieu Remazeilles

The University of Manchester

with H. K. Eriksen, I. K. Wehus

# Sky simulations 1: **PSM**

**CMB**

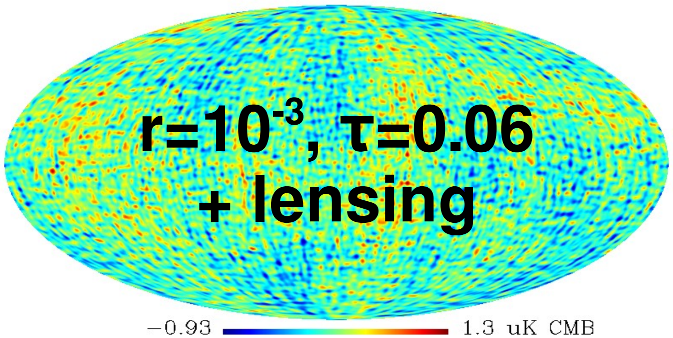


**Thermal dust @353 GHz**

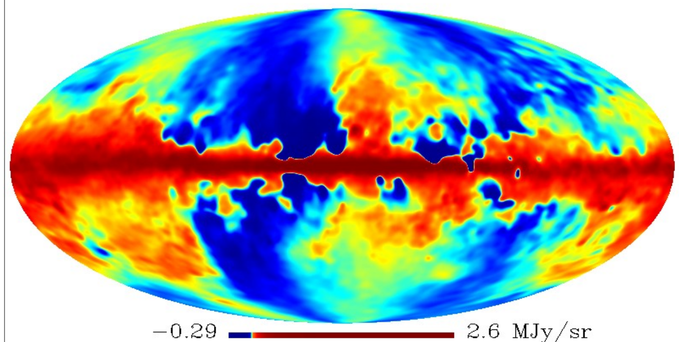


**Synchrotron @23 GHz**

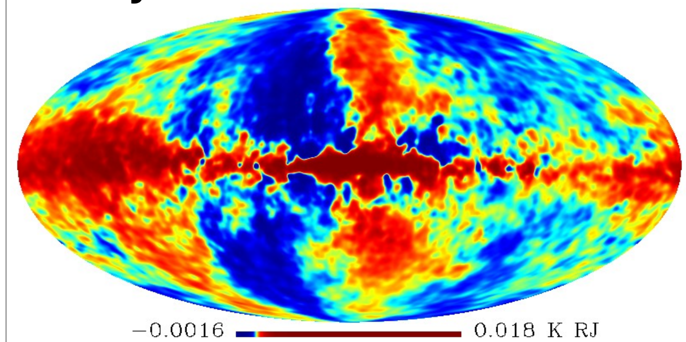


"Simple" sky:

- dust: modified blackbody
- synchrotron: curved power-law
- CMB: $r = 10^{-3}$ + lensing

dust spectral index

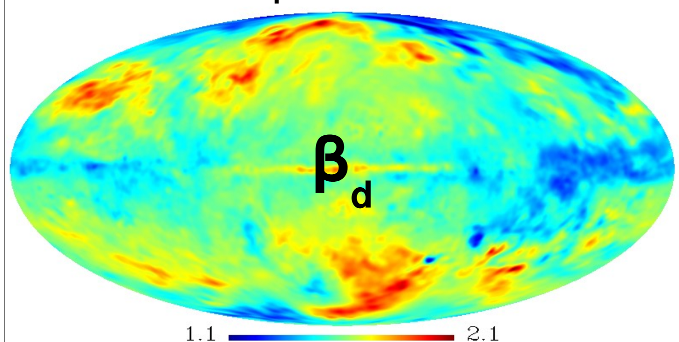


synchrotron spectral index

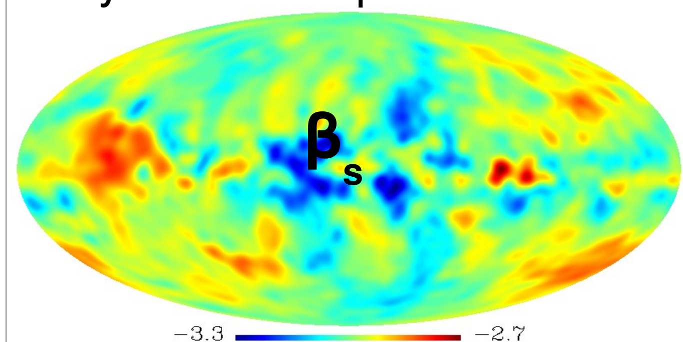


dust temperature

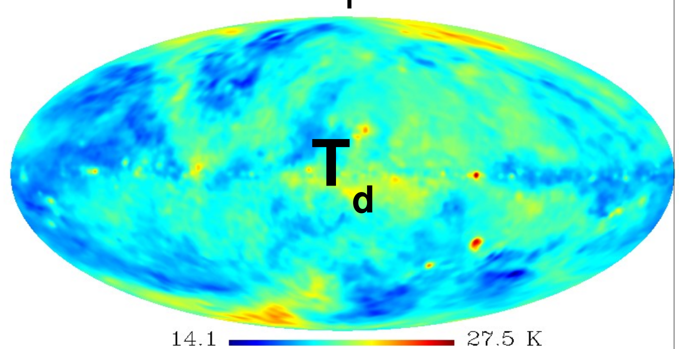


Synchrotron curvature

$C_s = 0.3$

***The PSM tool has been widely used and validated for many years by the Planck collaboration***

*smoothed to 1 degree for illustration purposes*

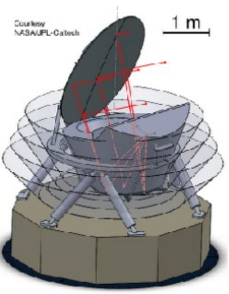


# PICO v2-1.4

## 21- 800 GHz

| | | | | | | |
|---|---|---|---|---|---|---|
| CMBP | | | | | | |
| del nu/nu | 0,25 | | del center | 1,2 | | |
| | | | | | | |
| nu1 | 30 | GHz | | | | |
| **Band#** | **nu (GHz)** | **nu_low (GHz)** | **nu_high (GHz)** | **del nu (GHz)** | **FWHM (arcmin)** | **PolWeight (uk*arcmin)** |
| 1 | 21 | 18,2 | 23,4 | 5,2 | 40,9 | 50 |
| 2 | 25 | 21,9 | 28,1 | 6,3 | 34,1 | 33 |
| 3 | 30 | 26,3 | 33,8 | 7,5 | 28,4 | 22,4 |
| 4 | 36,0 | 31,5 | 40,5 | 9,0 | 23,7 | 15 |
| 5 | 43,2 | 37,8 | 48,6 | 10,8 | 19,7 | 9,1 |
| 6 | 51,8 | 45,4 | 58,3 | 13,0 | 16,4 | 7 |
| 7 | 62,2 | 54,4 | 70,0 | 15,6 | 13,7 | 5 |
| 8 | 74,6 | 65,3 | 84,0 | 18,7 | 11,4 | 4 |
| 9 | 89,6 | 78,4 | 100,8 | 22,4 | 9,5 | 3,2 |
| 10 | 107,5 | 94,1 | 120,9 | 26,9 | 7,9 | 2,9 |
| 11 | 129,0 | 112,9 | 145,1 | 32,2 | 6,6 | 2,7 |
| 12 | 154,8 | 135,4 | 174,1 | 38,7 | 5,5 | 2,6 |
| 13 | 185,8 | 162,5 | 209,0 | 46,4 | 4,6 | 3,6 |
| 14 | 222,9 | 195,0 | 250,8 | 55,7 | 3,8 | 5,3 |
| 15 | 267,5 | 234,0 | 300,9 | 66,9 | 3,2 | 9 |
| 16 | 321,0 | 280,9 | 361,1 | 80,2 | 2,7 | 16,0 |
| 17 | 385,2 | 337,0 | 433,3 | 96,3 | 2,2 | 32 |
| 18 | 462,2 | 404,4 | 520,0 | 115,6 | 1,8 | 75 |
| 19 | 554,7 | 485,3 | 624,0 | 138,7 | 1,5 | 220,0 |
| 20 | 665,6 | 582,4 | 748,8 | 166,4 | 1,3 | 1100 |
| 21 | 798,7 | 698,9 | 898,5 | 199,7 | 1,1 | 10000,0 |

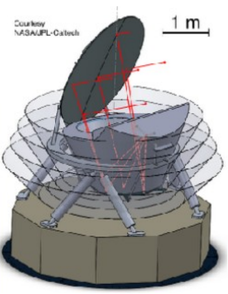


# PICO v3.0

## 21- 800 GHz

### *Increased sensitivities!*

| Band# | nu (GHz) | nu_low (GHz) | nu_high (GHz) | del nu (GHz) | FWHM (arcmin) | PolWeight (uK*arcmin) | Single bolometer NET (uK_CMB) |
|---|---|---|---|---|---|---|---|
| 1 | 21 | 18,2 | 23,4 | 5,2 | 38,4 | 16,3 | 94,7 |
| 2 | 25 | 21,9 | 28,1 | 6,3 | 32,0 | 11,7 | 86,6 |
| 3 | 30 | 26,3 | 33,8 | 7,5 | 28,3 | 7,8 | 54,9 |
| 4 | 36,0 | 31,5 | 40,5 | 9,0 | 23,6 | 5,6 | 50,2 |
| 5 | 43,2 | 37,8 | 48,6 | 10,8 | 22,2 | 5,4 | 40,3 |
| 6 | 51,8 | 45,4 | 58,3 | 13,0 | 18,4 | 4,0 | 37,1 |
| 7 | 62,2 | 54,4 | 70,0 | 15,6 | 12,8 | 3,9 | 56,5 |
| 8 | 74,6 | 65,3 | 84,0 | 18,7 | 10,7 | 3,2 | 52,7 |
| 9 | 89,6 | 78,4 | 100,8 | 22,4 | 9,5 | 2,0 | 33,8 |
| 10 | 107,5 | 94,1 | 120,9 | 26,9 | 7,9 | 1,7 | 32,1 |
| 11 | 129,0 | 112,9 | 145,1 | 32,3 | 7,4 | 1,6 | 26,7 |
| 12 | 154,8 | 135,4 | 174,1 | 38,7 | 6,2 | 1,4 | 26,3 |
| 13 | 185,8 | 162,5 | 209,0 | 46,5 | 4,3 | 2,5 | 49,9 |
| 14 | 222,9 | 195,0 | 250,8 | 55,7 | 3,6 | 3,1 | 56,0 |
| 15 | 267,5 | 234,0 | 300,9 | 66,9 | 3,2 | 2,0 | 41,7 |
| 16 | 321,0 | 280,9 | 361,1 | 80,3 | 2,6 | 3,0 | 55,3 |
| 17 | 385,2 | 337,0 | 433,3 | 96,3 | 2,5 | 3,3 | 69,0 |
| 18 | 462,2 | 404,4 | 520,0 | 115,6 | 2,1 | 7,8 | 141,0 |
| 19 | 554,7 | 485,3 | 624,0 | 138,7 | 1,5 | 44,1 | 460,5 |
| 20 | 665,6 | 582,4 | 748,8 | 166,4 | 1,3 | 176,9 | 1826,0 |
| 21 | 798,7 | 698,9 | 898,5 | 199,7 | 1,1 | 1260,7 | 10806,1 |

# Methodology

Eriksen et al 2004, 2008
Remazeilles et al 2016, 2017

**1.** Separation of components (`COMMANDER` fitting + Gibbs sampling):

$$\boldsymbol{s}^{(i+1)} \leftarrow P\left(\boldsymbol{s} | C_\ell^{(i)}, \boldsymbol{\beta}^{(i)}, \boldsymbol{d}\right),$$ *amplitudes (CMB, foregrounds)*

$$C_\ell^{(i+1)} \leftarrow P\left(C_\ell | \boldsymbol{s}^{(i+1)}\right),$$ *power spectrum (CMB)*

$$\boldsymbol{\beta}^{(i+1)} \leftarrow P\left(\boldsymbol{\beta} | \boldsymbol{s}^{(i+1)}, \boldsymbol{d}\right),$$ *spectral indices (foregrounds)*

**2.** Likelihood estimation of **r** and **A** $_{\mathbf{lens}}$:

$$-2 \ln \mathcal{L}\left[\widehat{C}_\ell | C_\ell^{th}(r, A_{lens})\right] = \sum_\ell (2\ell+1)\left[\ln\left(\frac{C_\ell^{th}}{\widehat{C}_\ell}\right) + \frac{C_\ell^{th}}{\widehat{C}_\ell} - 1\right]$$

$$C_\ell^{th} = r\, C_\ell^{tensor}(r=1) + A_{lens}\, C_\ell^{lensing}(r=0).$$

**3.** Blackwell-Rao posterior: $\mathcal{P}(r, A_{lens}) \approx \frac{1}{N}\sum_{i=1}^{N} \mathcal{L}\left[\widehat{C}_\ell^i | C_\ell^{th}(r, A_{lens})\right]$

***The Commander algorithm has strong heritage from real Planck data analysis***

# Commander reconstruction of CMB E-modes
# 21 – 800 GHz

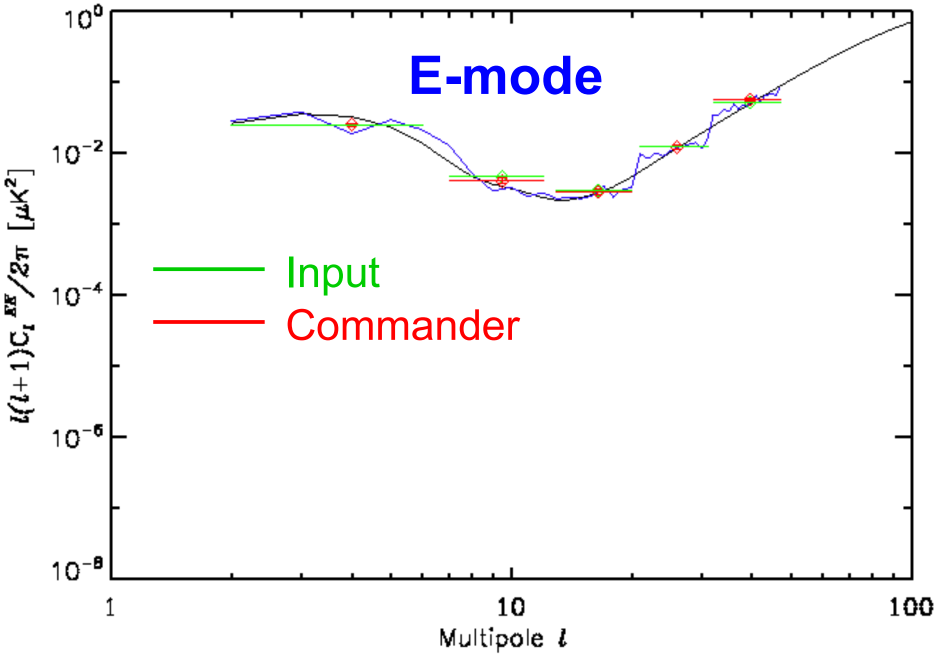


**$\tau = 0.0607 \pm 0.0023$**

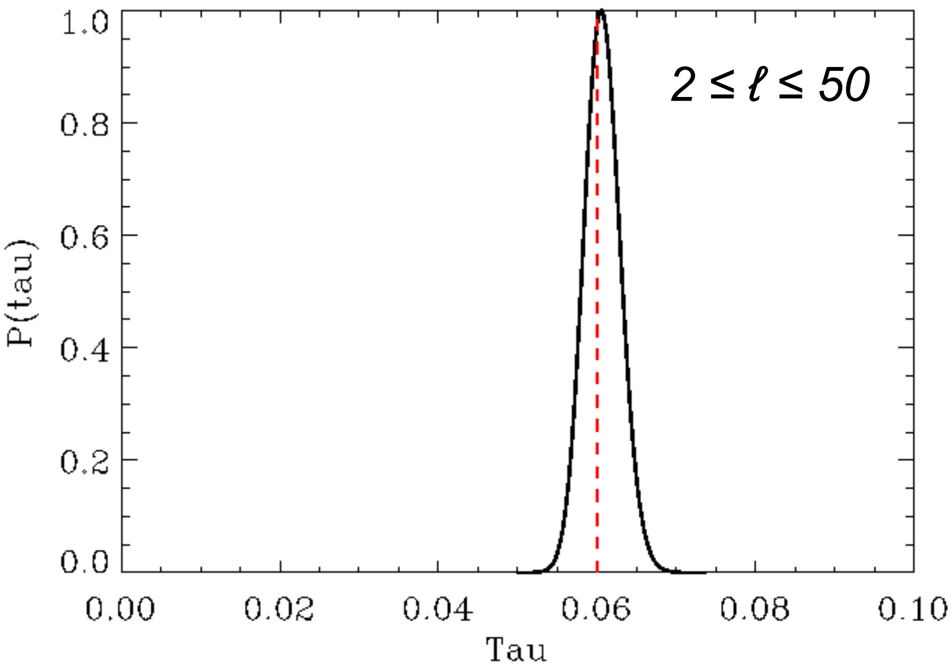


*Foregrounds:*

- *Synchrotron power-law with curvature: $\beta_s$ , $C_s$*
- *Thermal dust MBB: $\beta_d$, $T_d$*

***E-modes serve as a useful validation of the Commander algorithm***

*M. Remazeilles*

# Commander reconstruction of CMB B-modes
# 21 – 800 GHz

r = $10^{-3}$ + lensing, $f_{sky}$=50%

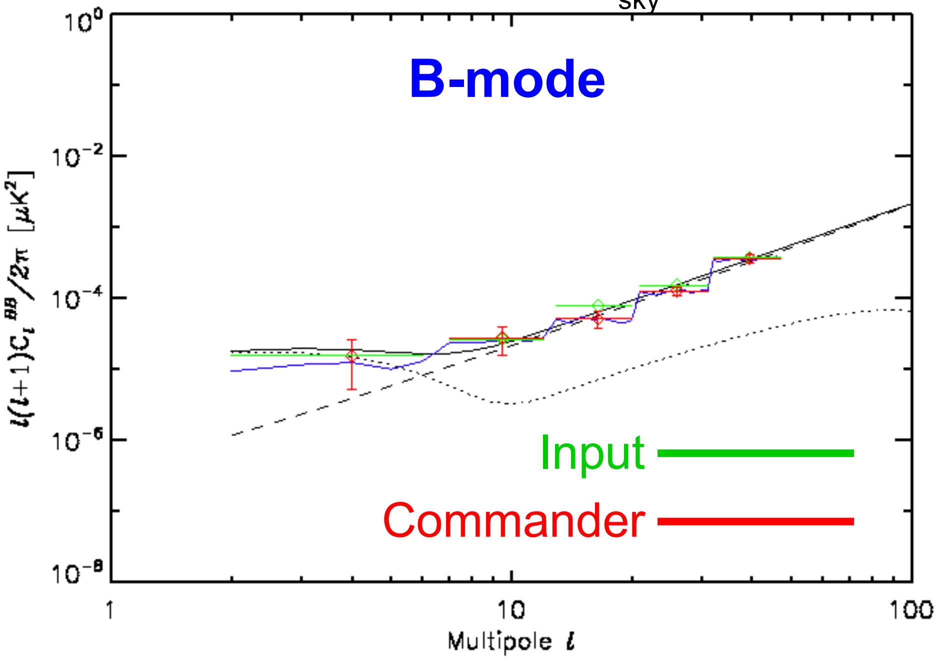


r = (0.30 ± 0.41) × $10^{-3}$

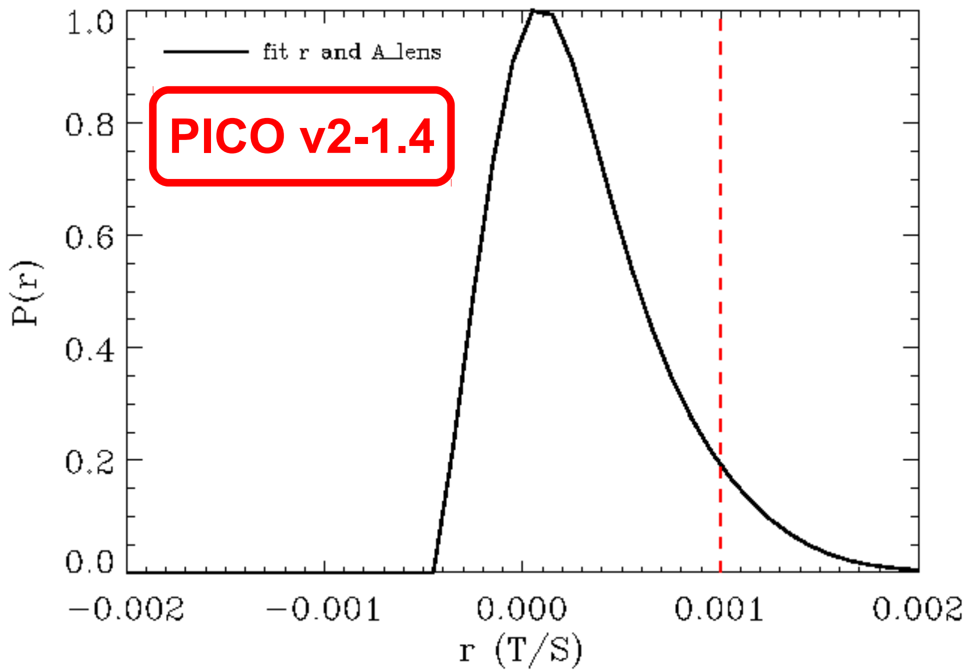


$2 \leq \ell \leq 50$

Foregrounds:

- *Synchrotron power-law with curvature: $\beta_s$ , $C_s$*
- *Thermal dust MBB: $\beta_d$, $T_d$*

$\beta_d$, $T_d$, $\beta_s$ locally fitted in each pixel
$C_s$ globally fitted

*M. Remazeilles*

# Commander reconstruction of CMB B-modes
# 21 – 800 GHz

r = $10^{-3}$ + lensing, $f_{sky}$=50%

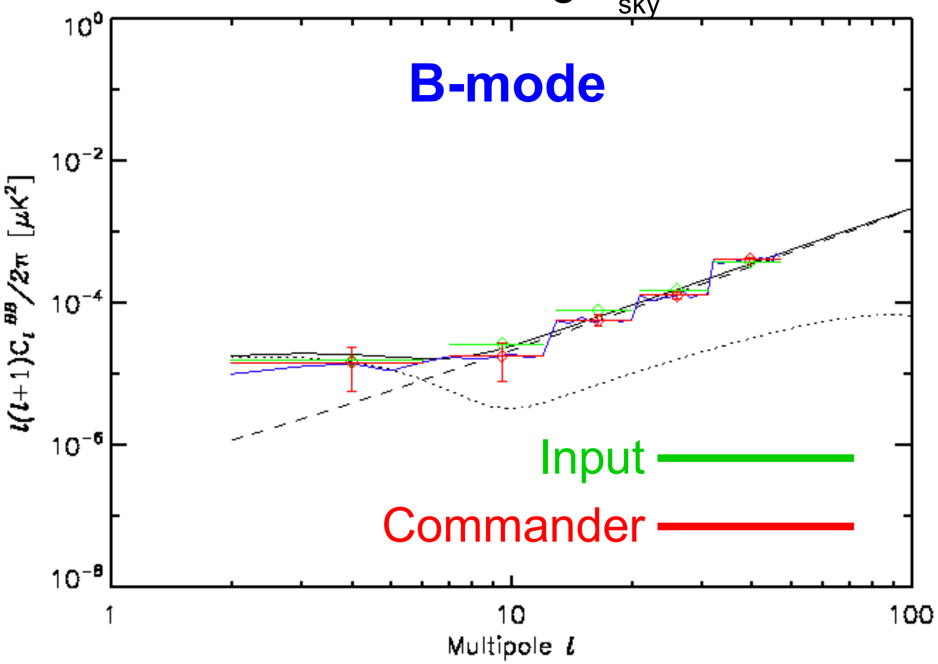


r = (0.51 ± 0.36) × $10^{-3}$

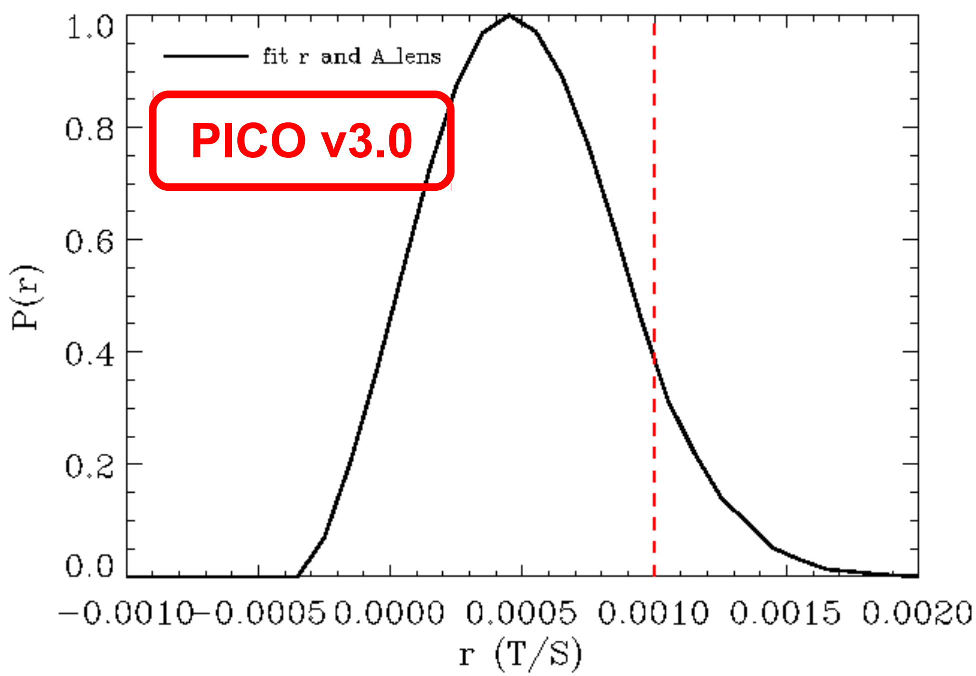


$2 \le \ell \le 50$

*Foregrounds:*

- *Synchrotron power-law with curvature: $\beta_s$ , $C_s$*
- *Thermal dust MBB: $\beta_d$, $T_d$*

$\beta_d$, $T_d$, $\beta_s$ locally fitted in each pixel
$C_s$ globally fitted

***Increased sensitivity reduces σ(r) by 10% only***

*M. Remazeilles*

# Commander results on foregrounds

# PICO v2-1.4

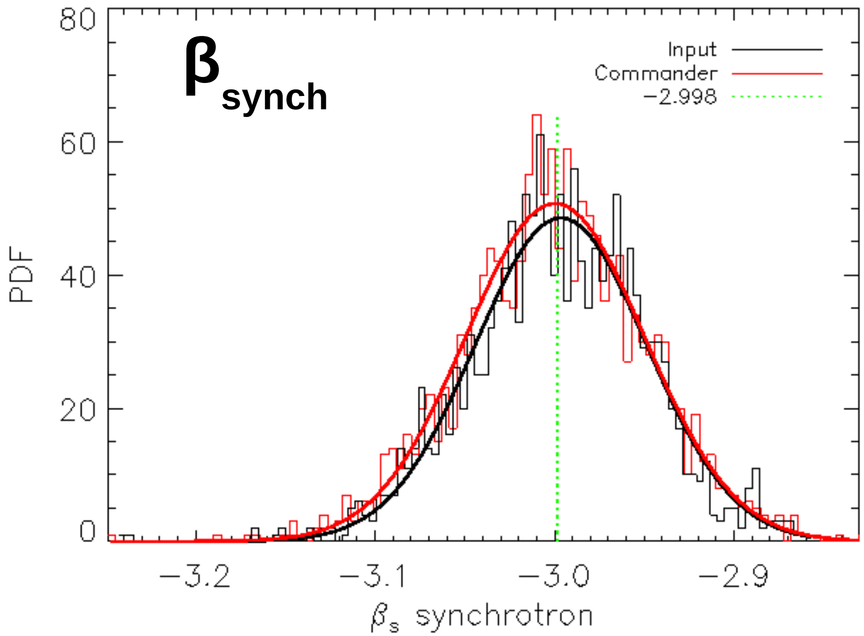


***Thanks to the broad frequency range of PICO, dust and synchrotron spectral parameters are all accurately recovered***

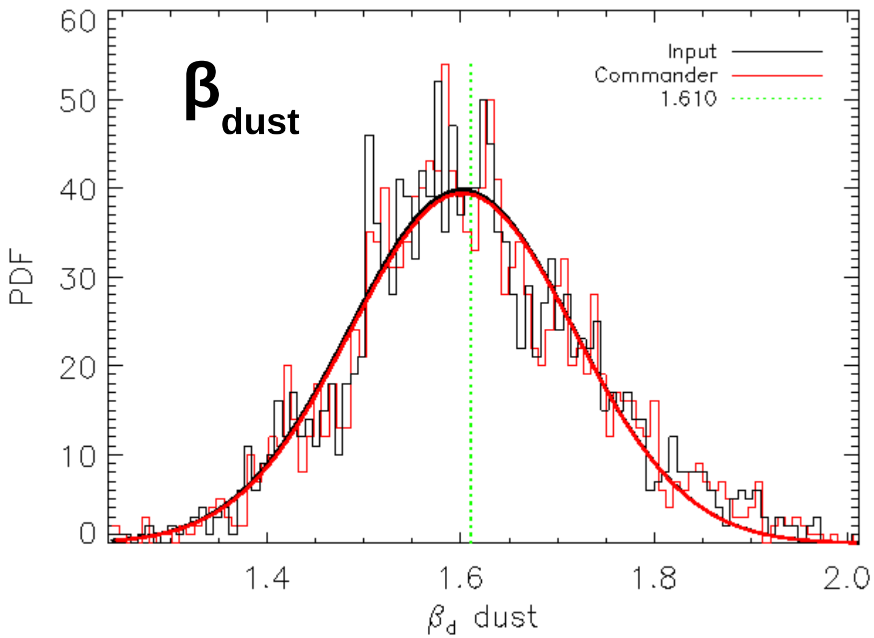


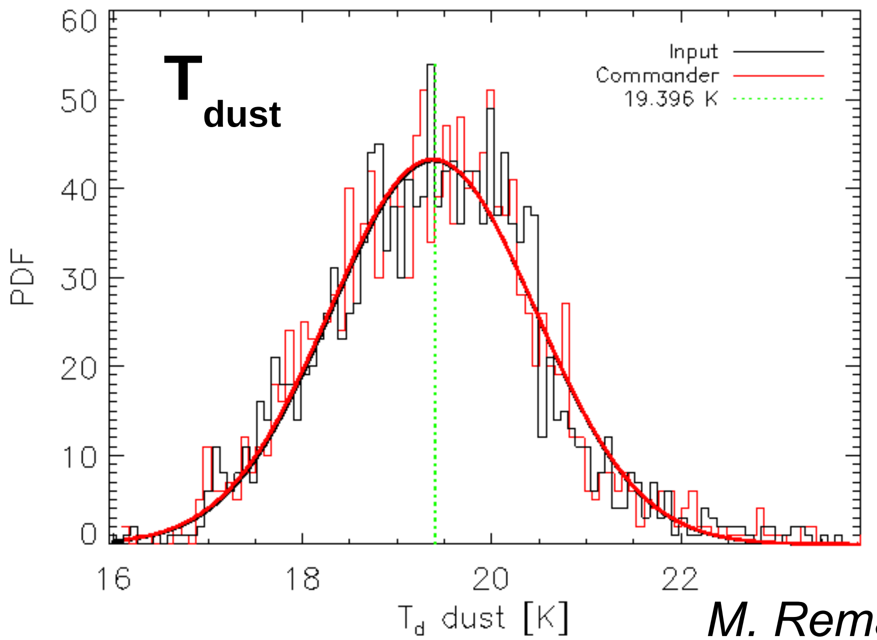


*M. Remazeilles*

# Commander results on foregrounds
# PICO v3.0

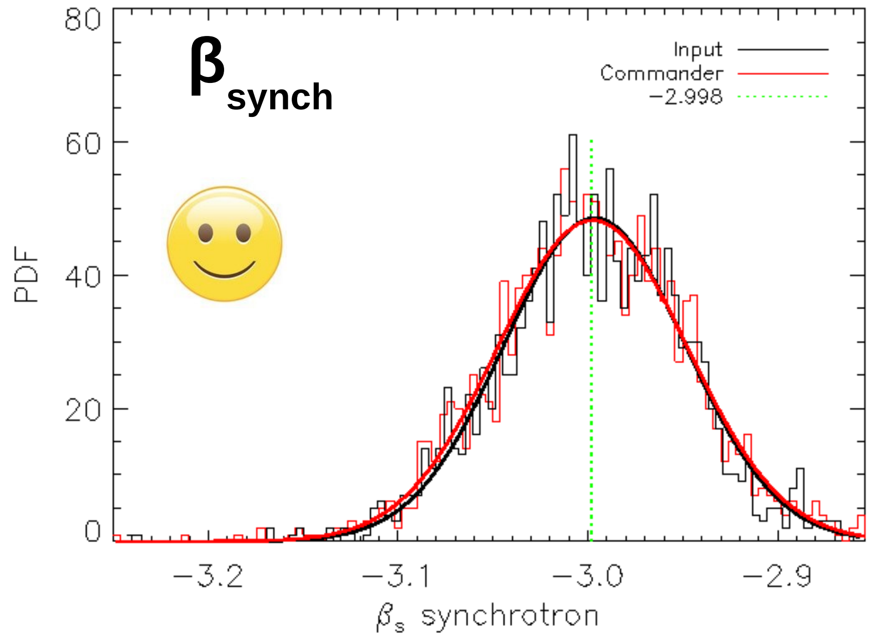


***Increased sensitivities of PICO v3.0 improve the constraints on the synchrotron spectral index***

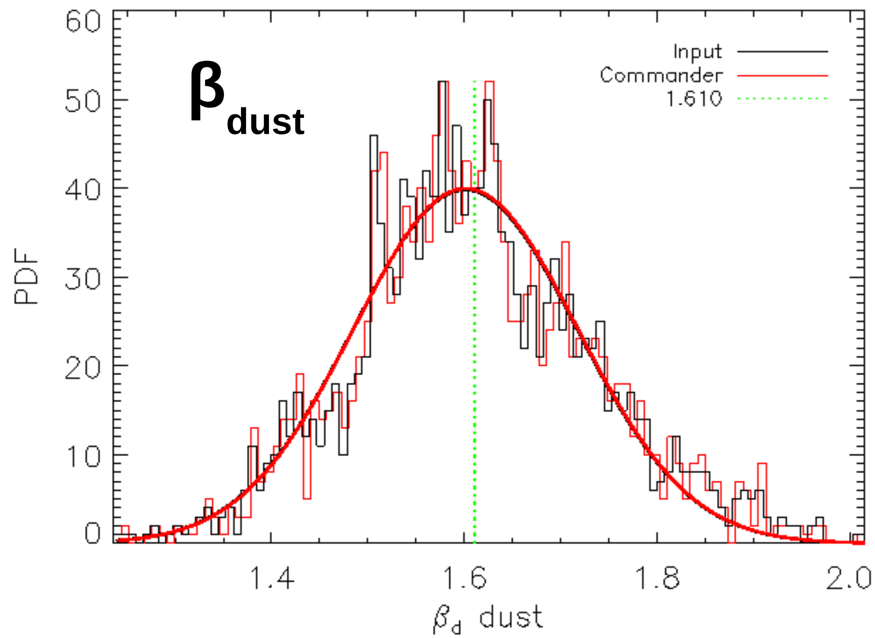


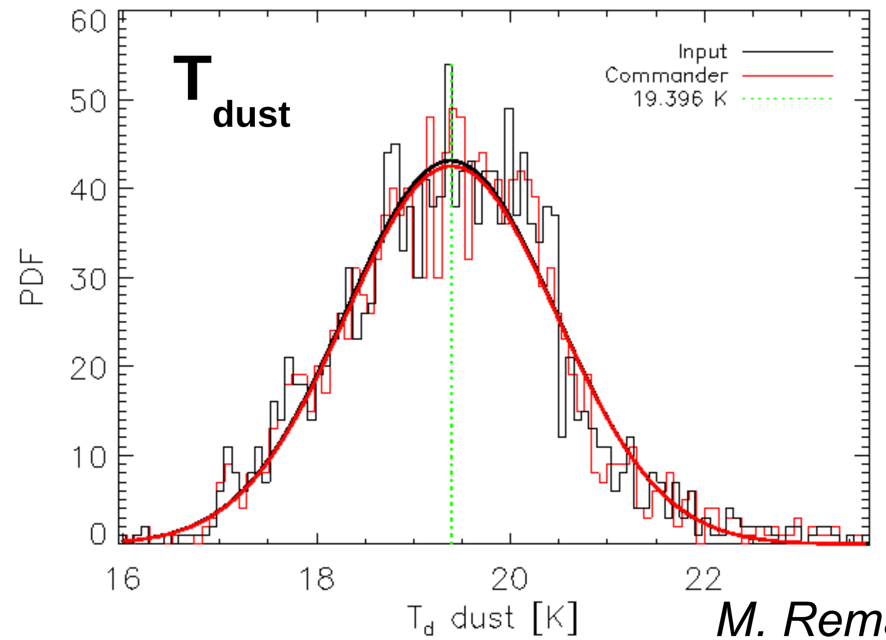


*M. Remazeilles*

# Commander reconstruction of CMB B-modes

# **No foregrounds, 50% mask**

*sample variance + noise (50% of the sky)*

r = $10^{-3}$ + lensing, $f_{sky}$=50%

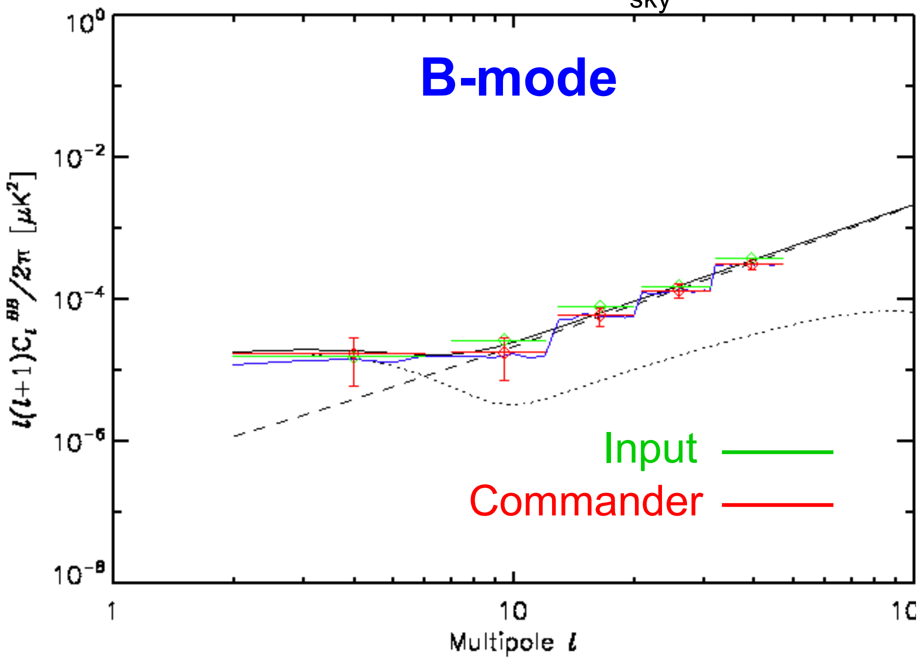


**r = (0.6 ± 0.4) × $10^{-3}$**

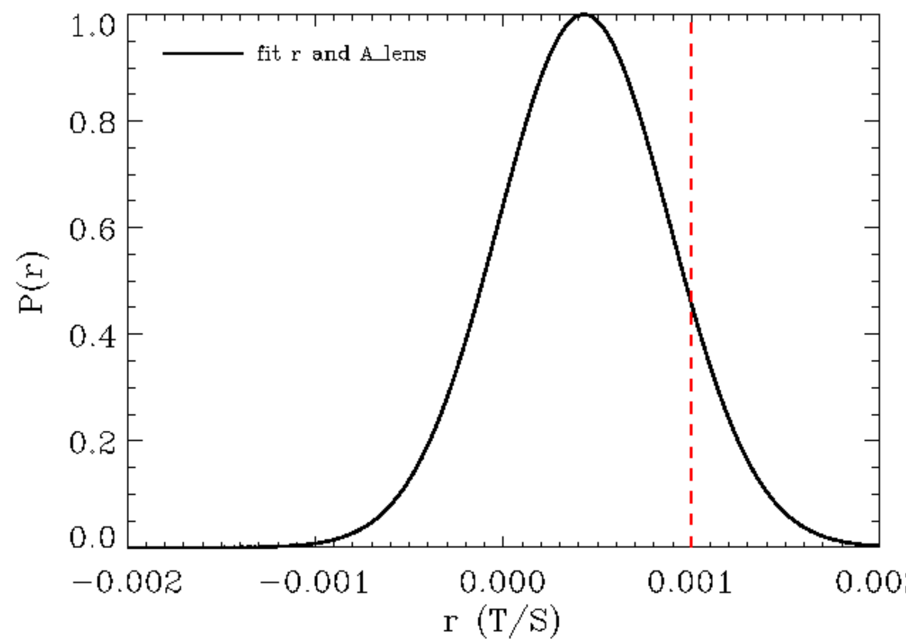


**Sample variance σ(r = $10^{-3}$) = 0.4 x $10^{-3}$**

*That's the minimal uncertainty that can be achieved from $2 \leq \ell \leq 50$ in the absence of foregrounds on 50% of the sky*

*M. Remazeilles*

# How σ(r) reduces after foreground cleaning and 60% delensing?

→ **60% delensing is the value quoted by CORE:**

**Challinor et al JCAP (2018), 1707.02259**

→ **Shortcut adopted for delensing:**

1. *The input CMB map is simulated from the "modified" power spectrum:*

$$C_\ell^{BB}(CMB) = C_\ell^{BB}(tensor) + 0.40 * C_\ell^{BB}(lensing)$$

2. *Foreground cleaning is then performed on the "modified" sky simulations*

*M. Remazeilles*

# Commander reconstruction of CMB B-modes
# no delensing

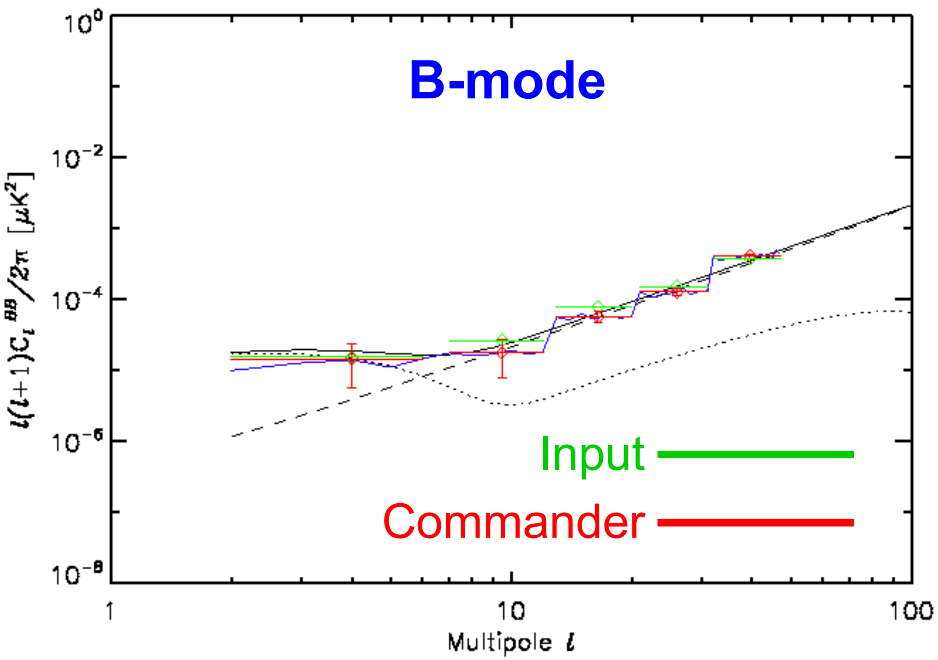


**r = (0.51 ± 0.36) × 10⁻³**

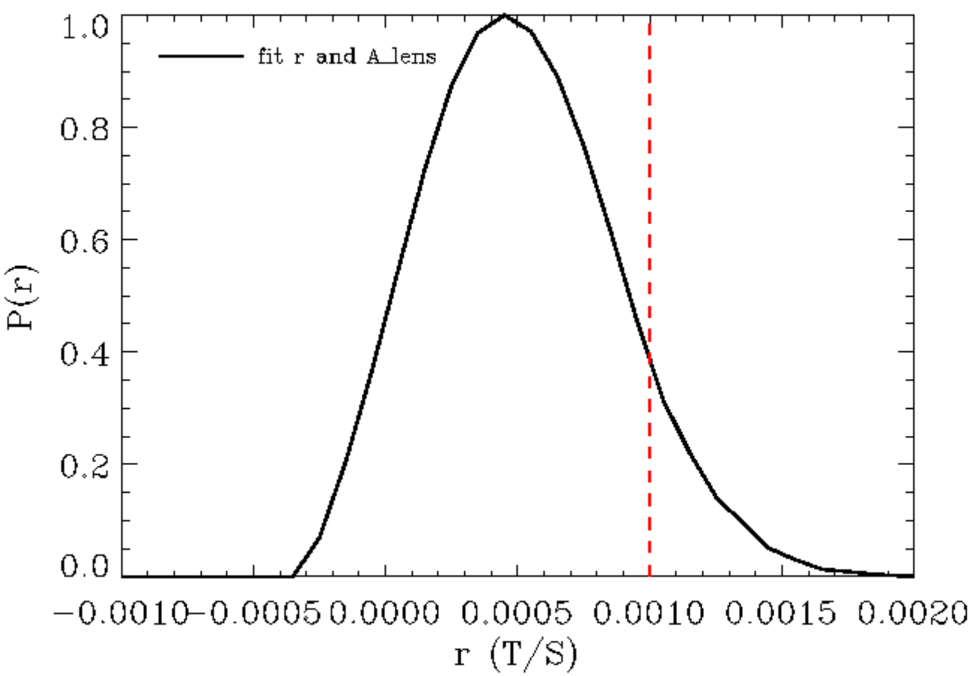


*$2 \leq \ell \leq 50$*

*<u>Foregrounds</u>:*

- *Synchrotron power-law with curvature: $\beta_s$ , $C_s$*
- *Thermal dust MBB: $\beta_d$, $T_d$*

*M. Remazeilles*

# Commander reconstruction of CMB B-modes
# 60% delensing

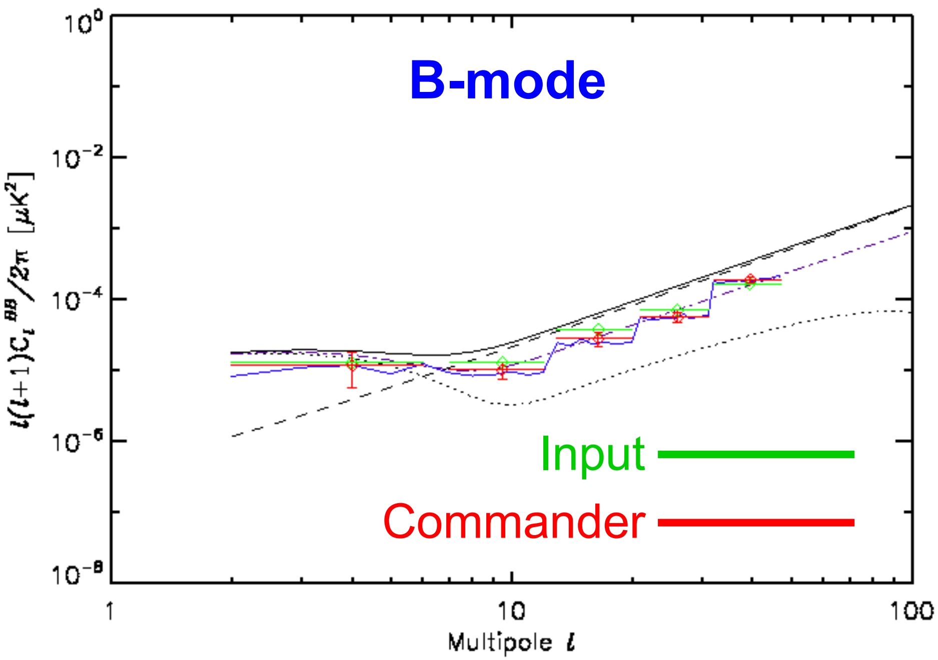


**r = (0.57 ± 0.24) × 10^-3**

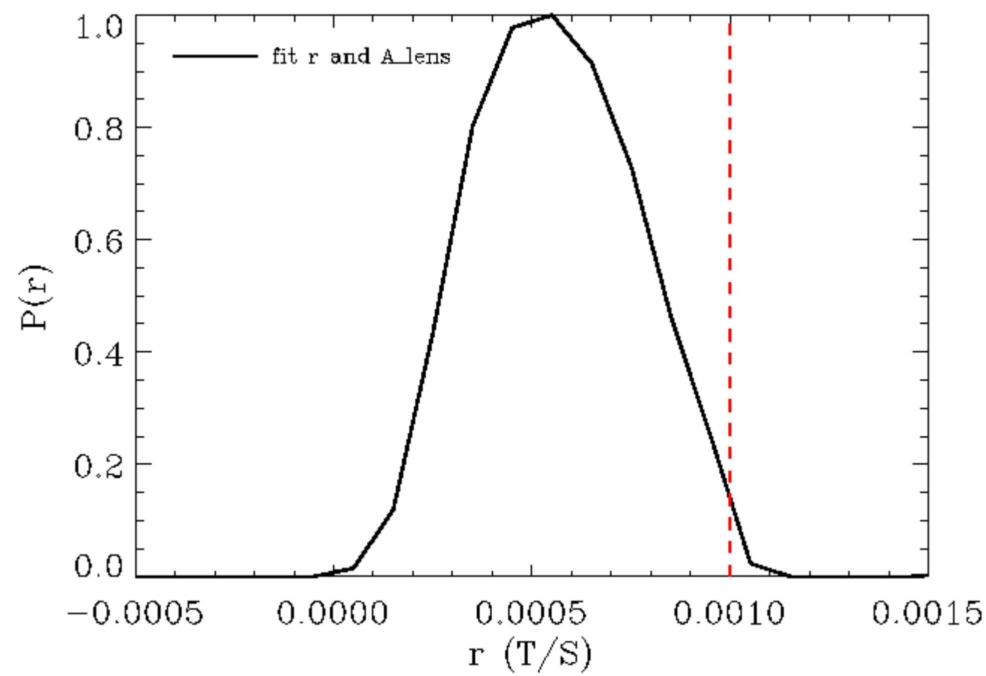


$2 \leq \ell \leq 50$

*Foregrounds*:

- *Synchrotron power-law with curvature: $\beta_s$ , $C_s$*
- *Thermal dust MBB: $\beta_d$, $T_d$*

*M. Remazeilles*

# Discarding PICO frequencies?

# Commander reconstruction of CMB B-modes

# 21 – 800 GHz

**r = $10^{-3}$**

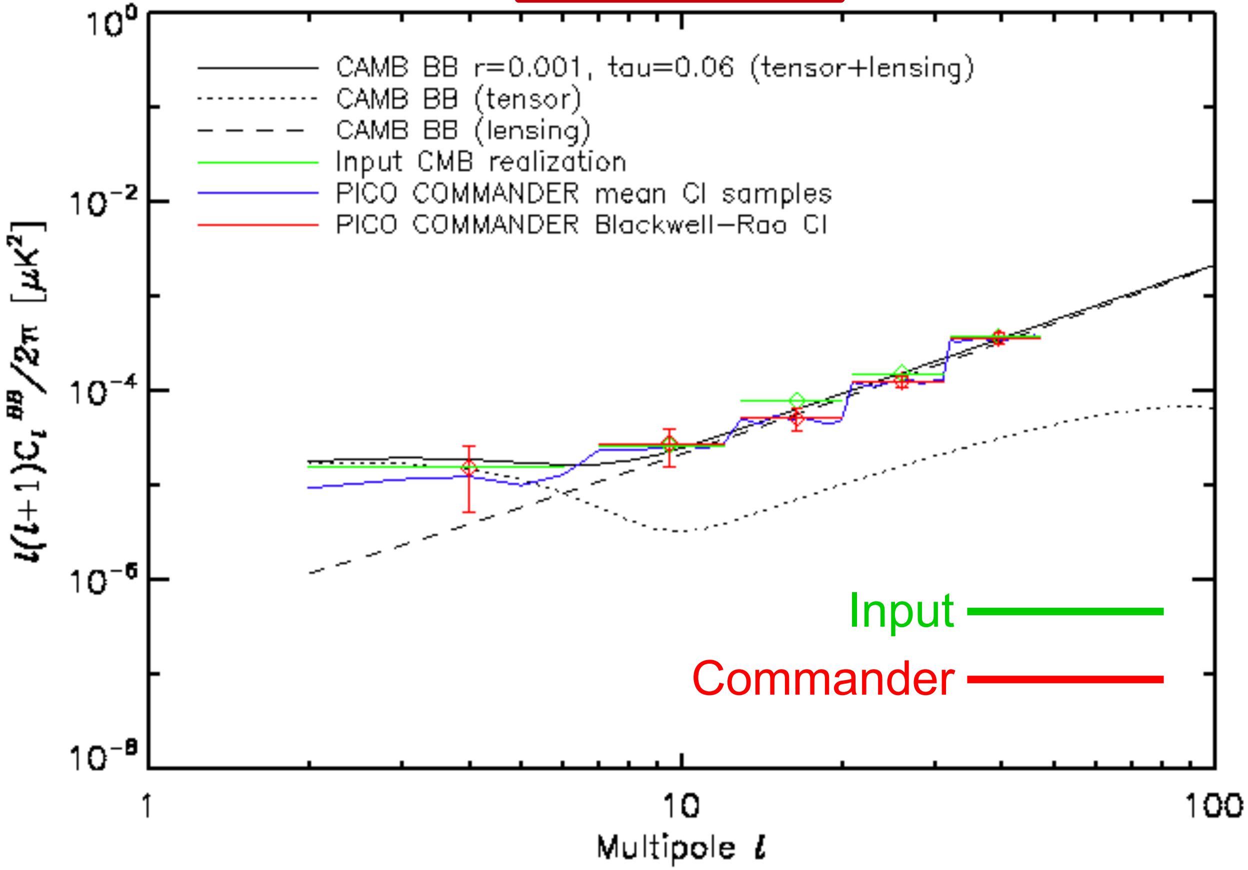


*Foregrounds*:

- *Synchrotron (power-law with curvature)*
- *Thermal dust (MBB)*

**σ(r = $10^{-3}$) = 0.4 x $10^{-3}$**

**after foreground cleaning**

*M. Remazeilles*

# Commander reconstruction of CMB B-modes

## 43 – 462 GHz

**$r = 10^{-3}$**

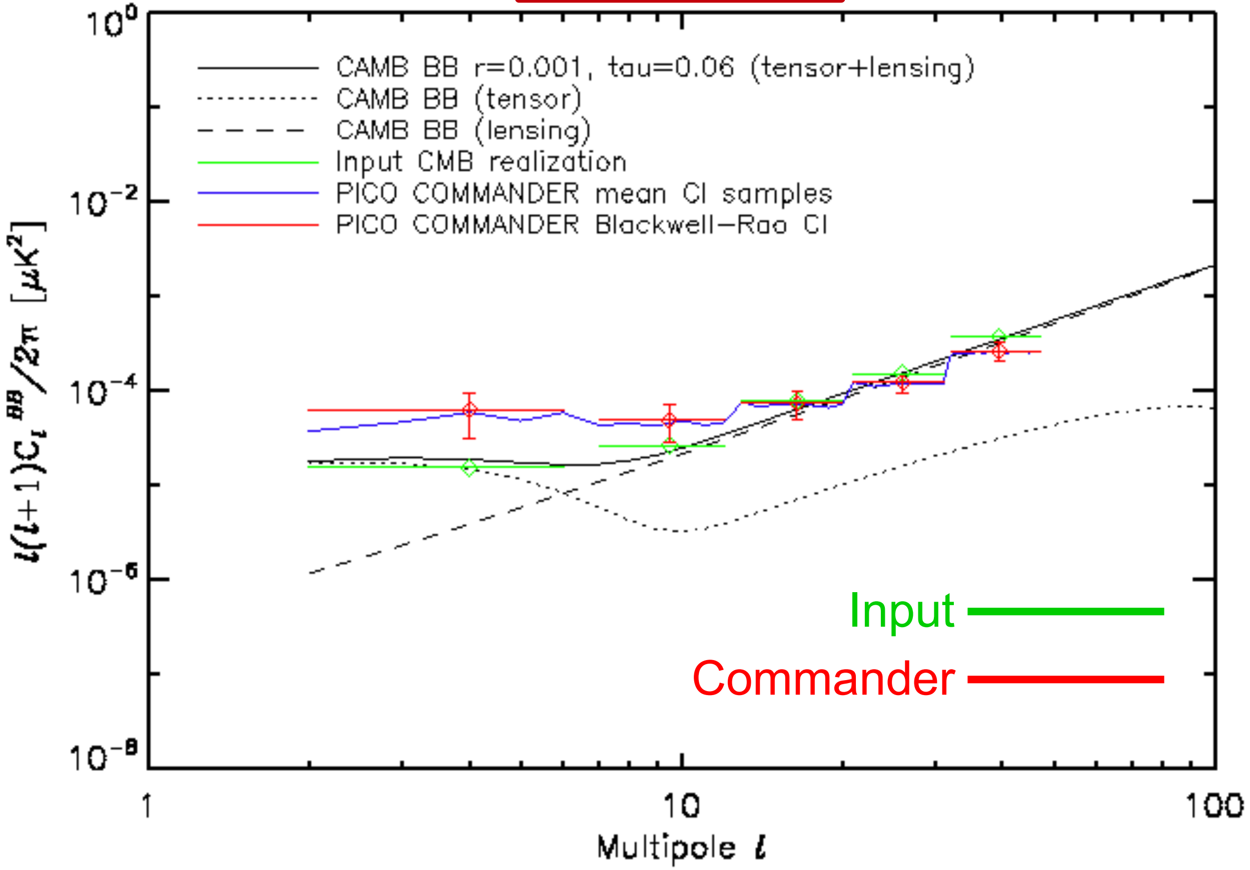


*Foregrounds*:

- *Synchrotron (power-law with curvature)*
- *Thermal dust (MBB)*

**Narrowing the frequency range of observations causes biases on large-scales due to foregrounds**

*M. Remazeilles*

# COMMANDER results on foregrounds
# PICO **21 – 800 GHz**

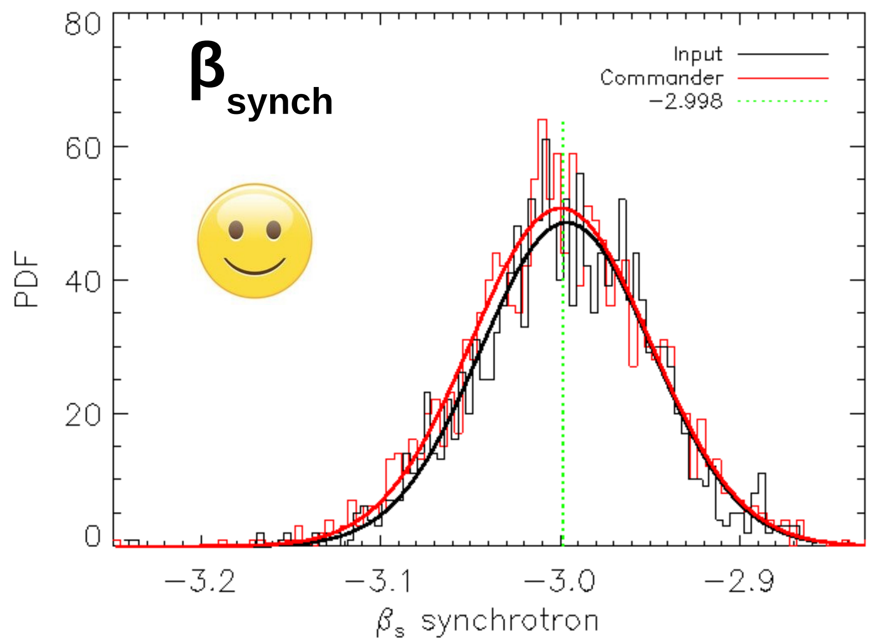


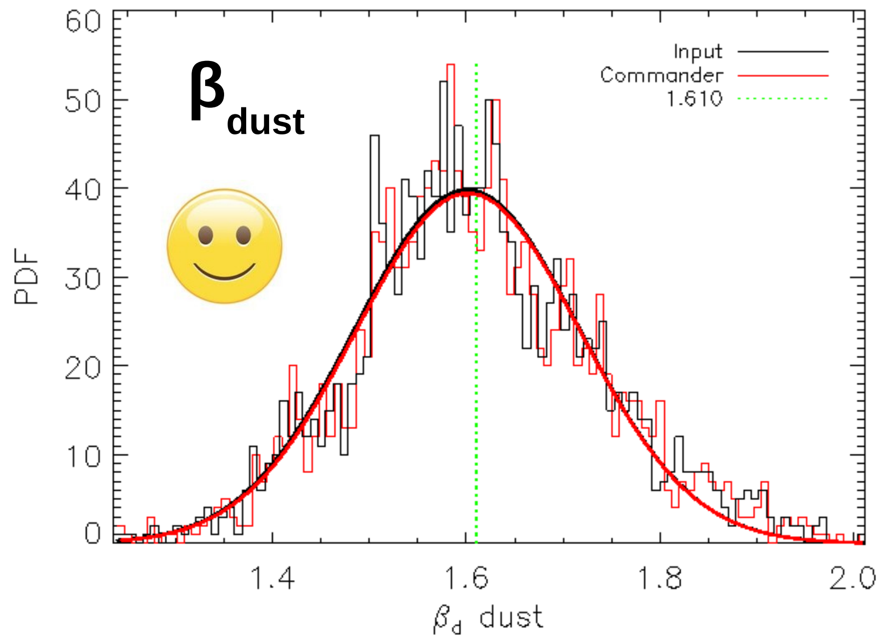


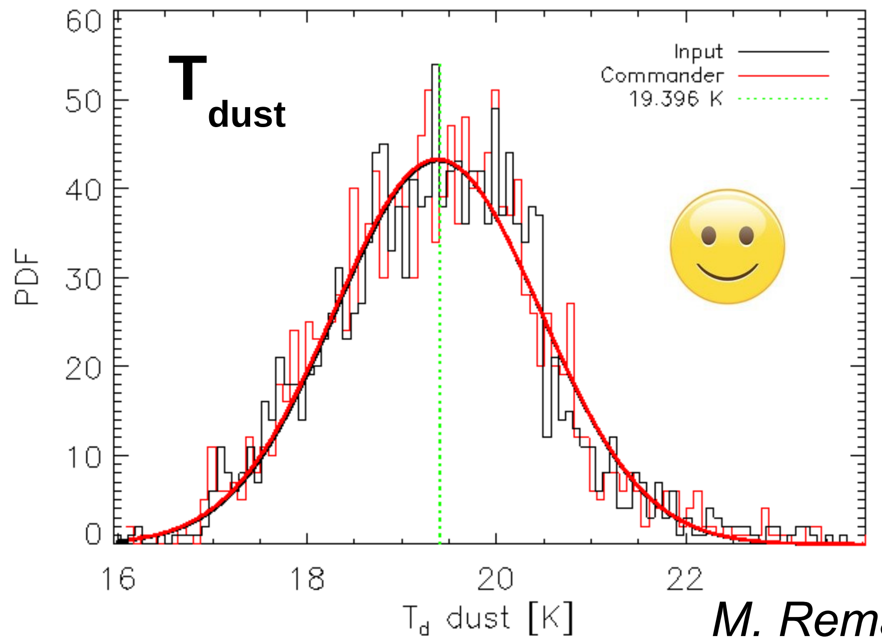


*M. Remazeilles*

# COMMANDER results on foregrounds
# PICO **43 – 462 GHz**

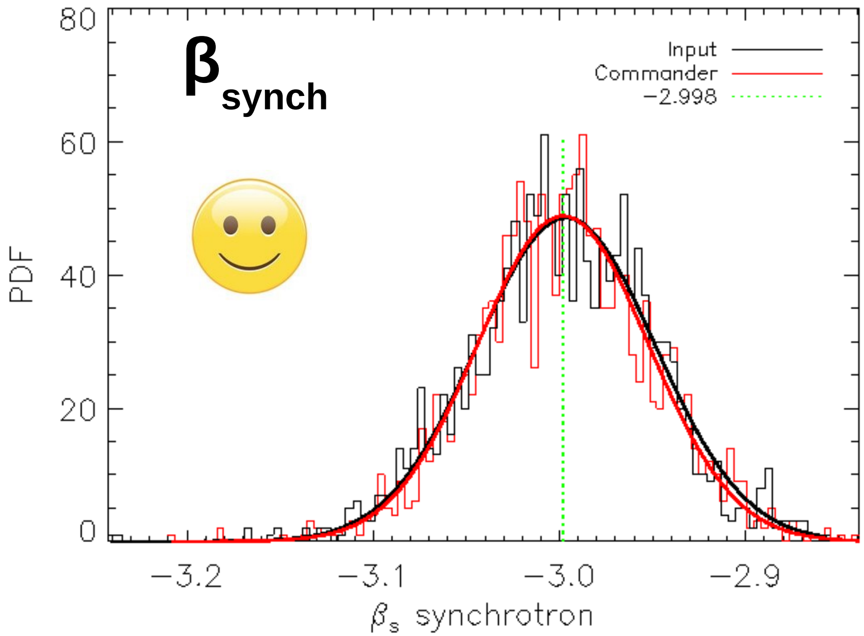


**Lack of frequency range / high frequencies**

**Lack of precision/constraint on $T_{dust}$**

**Translates into a bias on CMB B-mode by extrapolation towards CMB frequencies**

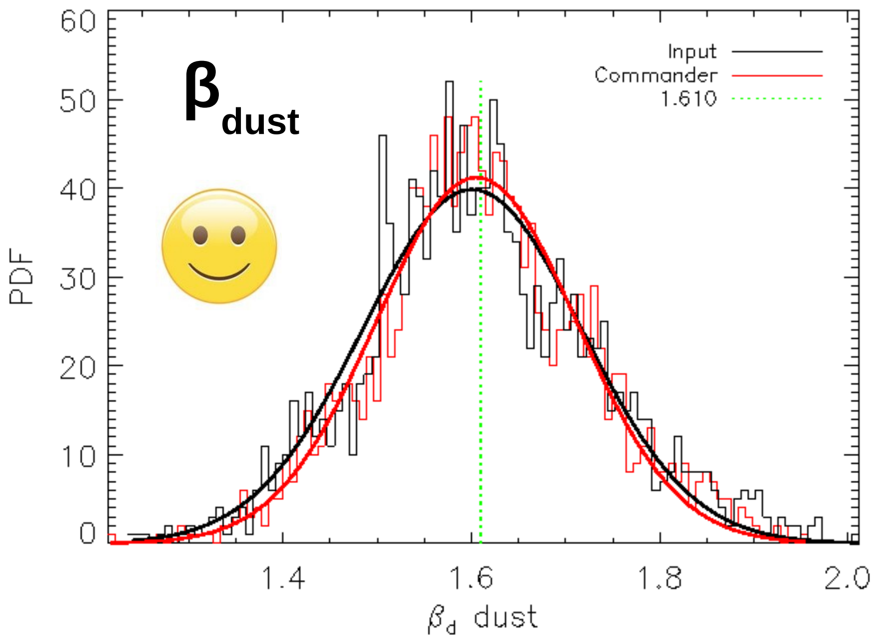


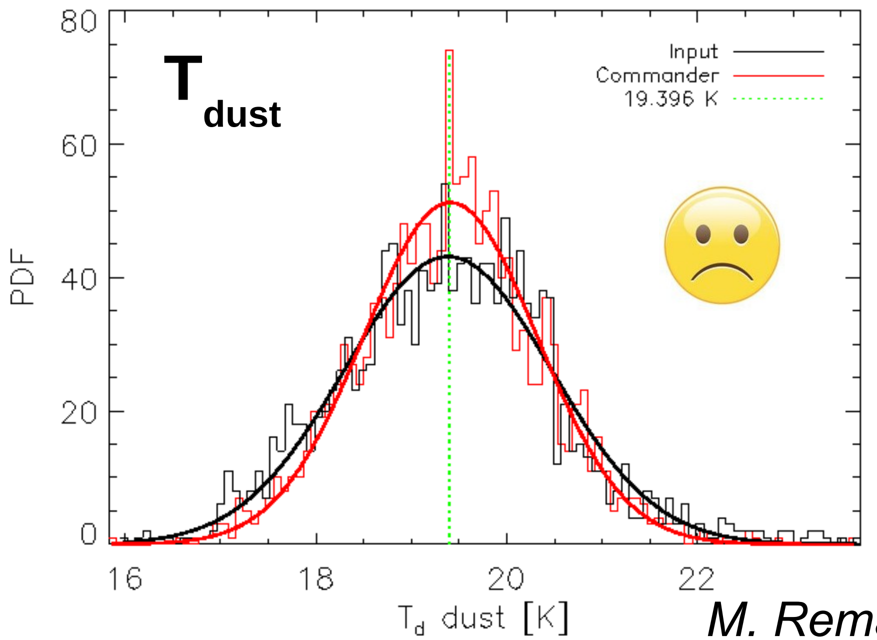


*M. Remazeilles*

# PICO
## 21 – 800 GHz

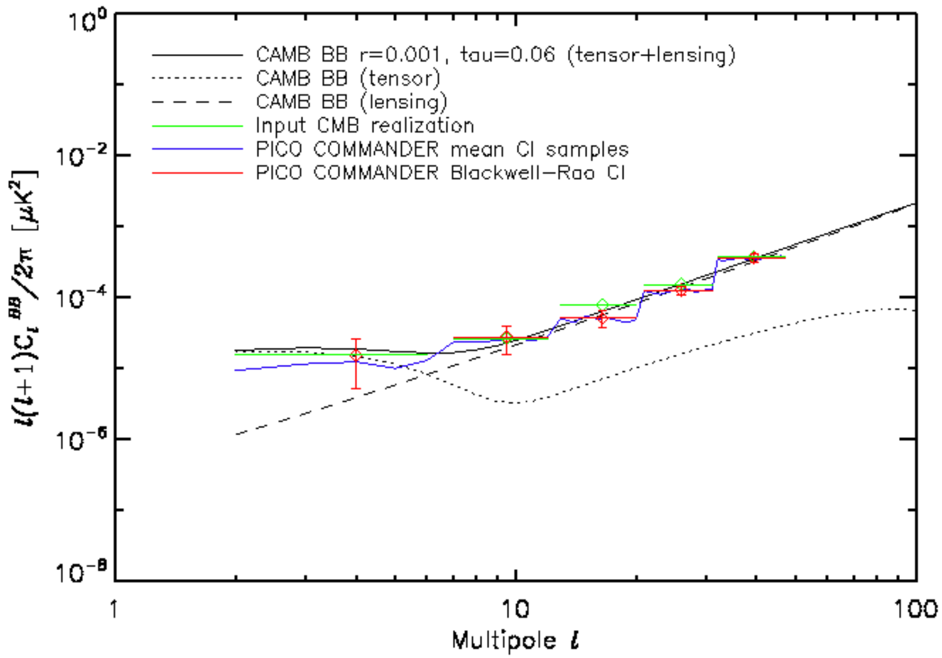


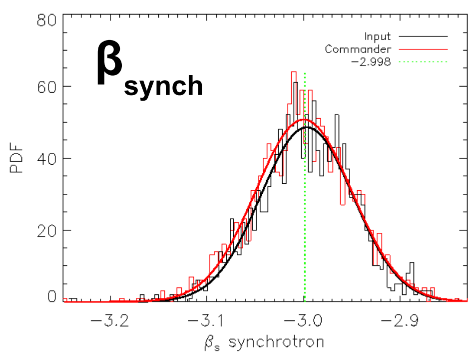


**σ(r=10$^{-3}$) = 0.4 × 10$^{-3}$**

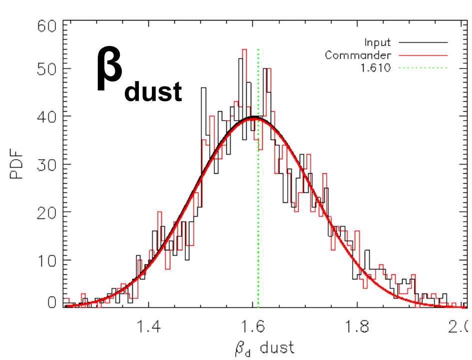


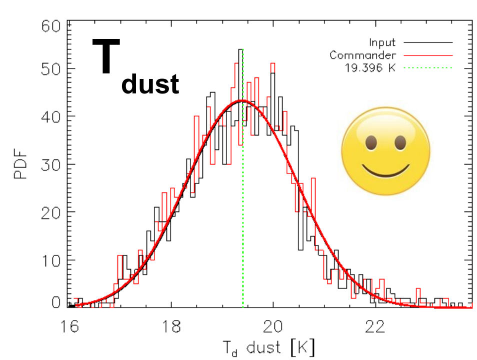


# PICO
## 43 – 462 GHz

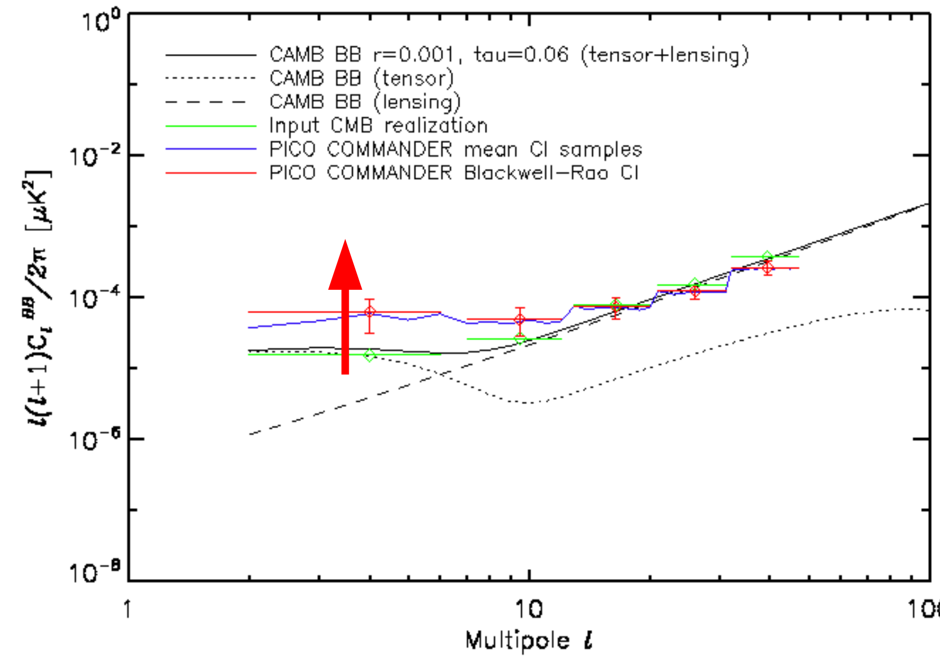


**σ(r=10$^{-3}$) = 0.7 × 10$^{-3}$**

**(75% increase)**

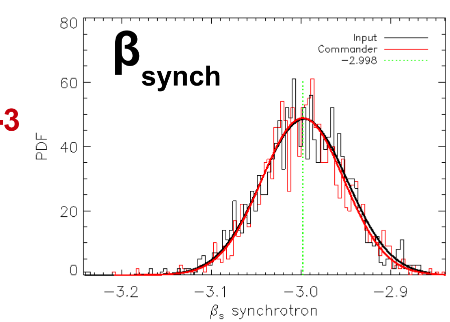


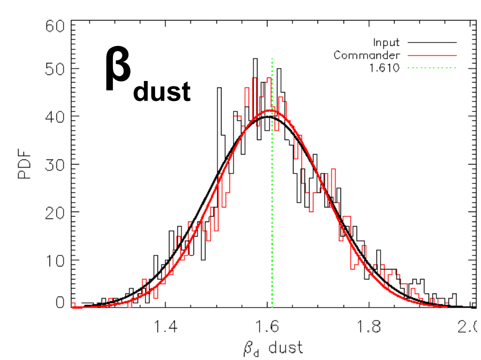


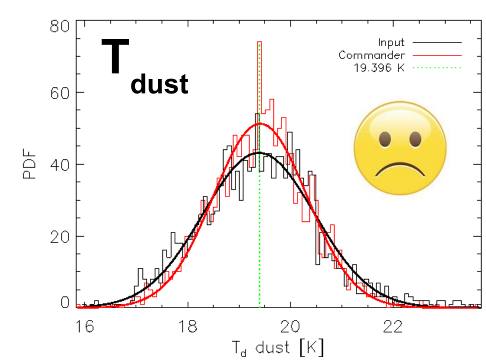

# PICO
## 21 – 800 GHz

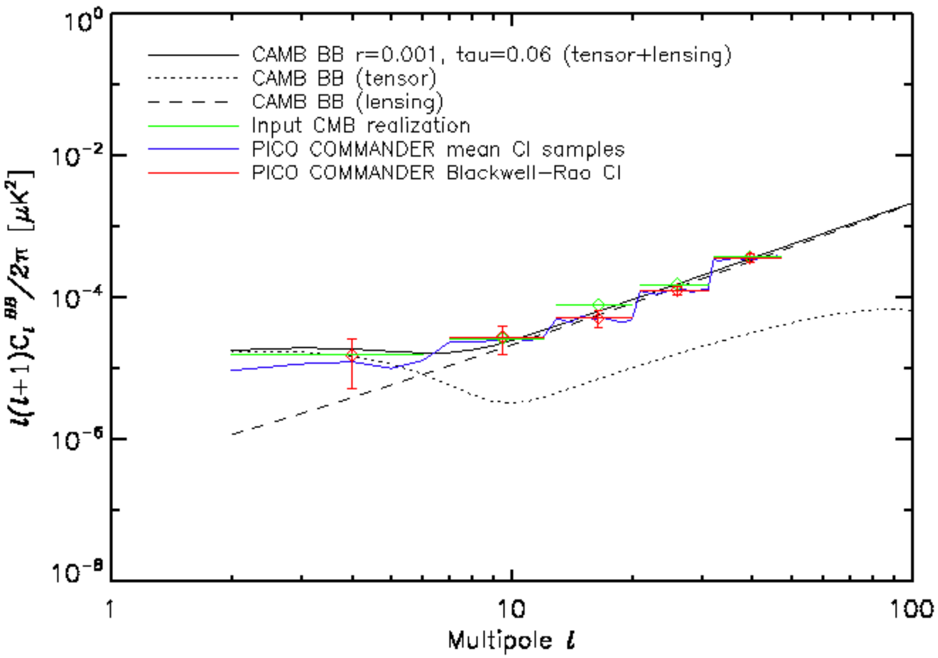


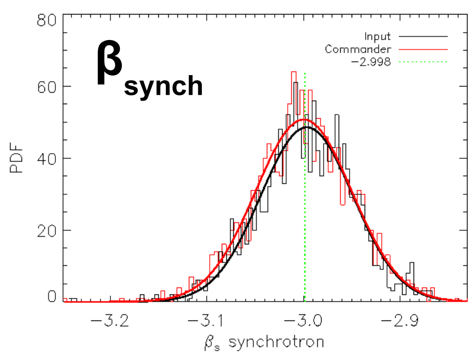


$\sigma(r=10^{-3}) = 0.4 \times 10^{-3}$

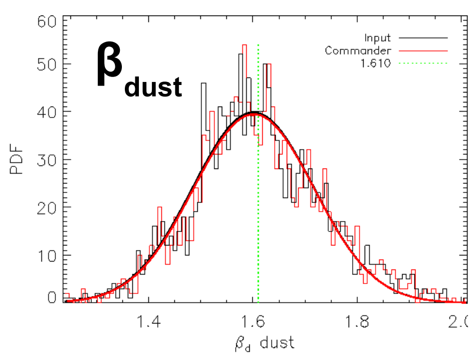


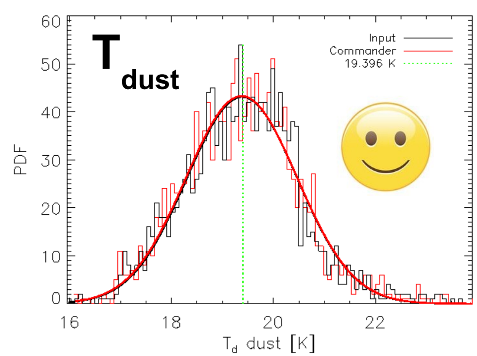


# PICO
## 43 – 800 GHz

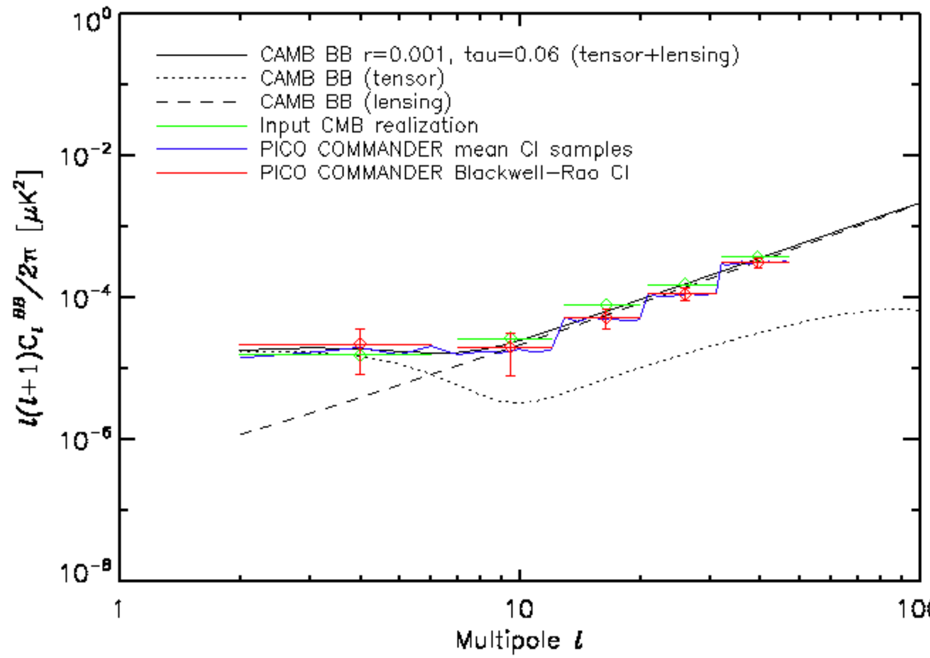


$\sigma(r=10^{-3}) = 0.5 \times 10^{-3}$

(25% increase)

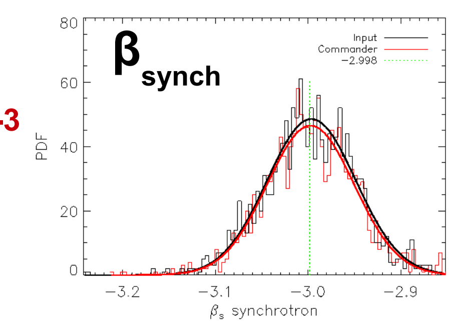


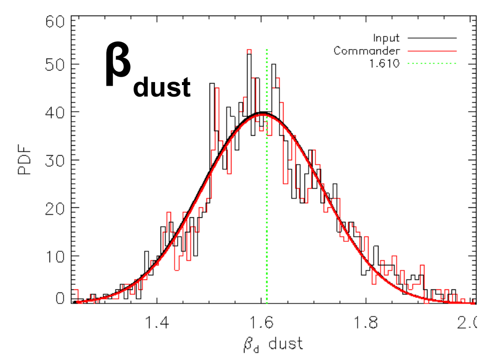


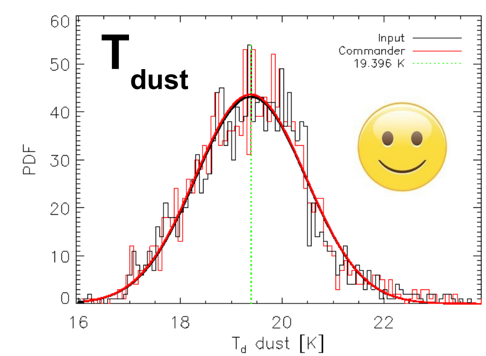

# Summary for PICO

| | estimated r [$\times 10^{-3}$] | $\sigma(r=10^{-3})$ [$\times 10^{-3}$] |
|---|---|---|
| • **21 – 800 GHz, no foregrounds, 50% mask** | 0.6 | **0.4** |
| | | |
| • **21 – 800 GHz, with foregrounds, 50% mask** | | |
| **PICO v2-1.4** | 0.30 | **0.41** |
| **PICO v3.0**<br>**PICO v3.0 + 60% delensing** | 0.51<br>0.57 | **0.36**<br>**0.24** |
| | | |
| • **43 – 800 GHz, with foregrounds, 50% mask** | 0.4 | **0.5** |
| • **43 – 462 GHz, with foregrounds, 50% mask** | 1.3 | **0.7** |

***These results are for $2 \leq \ell \leq 50$.***

***We should be able to reduce σ(r) by going to higher multipoles, e.g. by combining COMMANDER at low-ℓ and NILC/SEVEM at high-ℓ***

*M. Remazeilles*

# *Backup slides*

# #1. Foreground mismodelling

**Impact on r of mismodelling two MBB dust components as a single MBB component:**

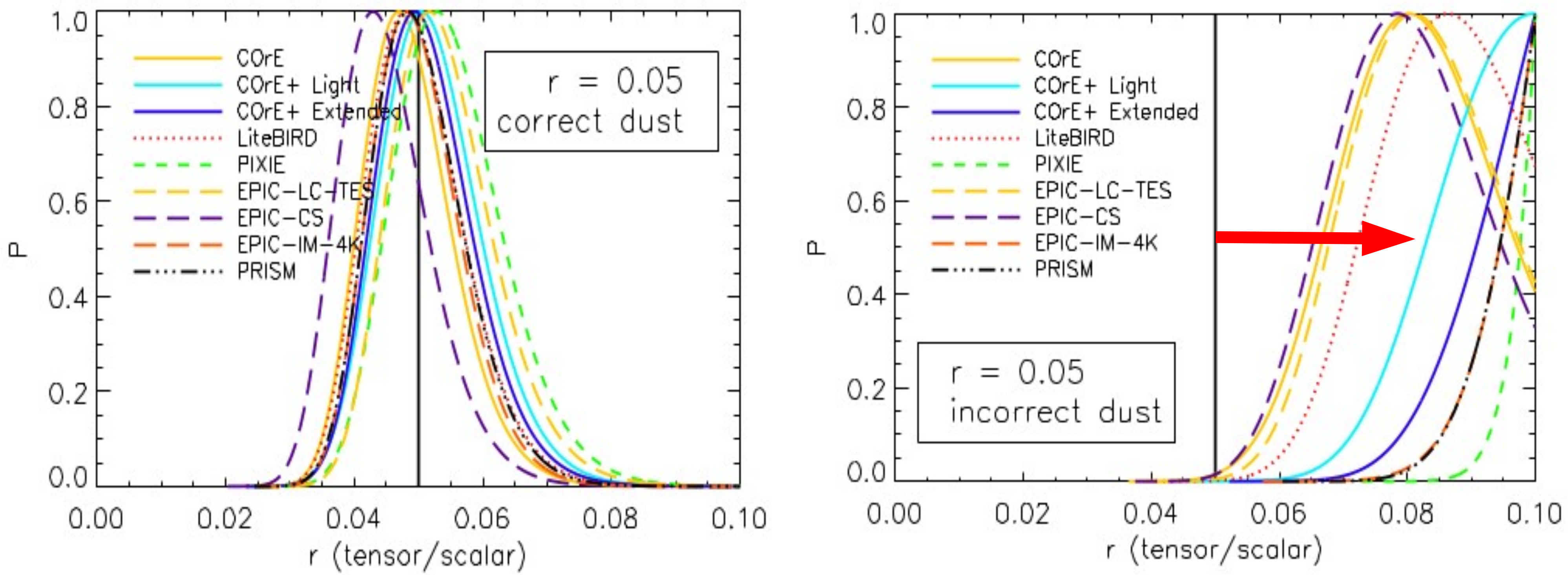


***Remazeilles, Dickinson, Eriksen, Wehus, MNRAS (2016)***

**<u>The Sneaky Point</u>:**

***CMB experiments with narrow frequency range < 400 GHz show no evidence ($\chi$2 ~ 1) for incorrect foreground modelling!***

# #2. Extragalactic compact foregrounds cannot be ignored

***Polarized Radio and IR compact sources at ~ 100 GHz dominate the primordial CMB B-mode at r = 10^-3 on angular scales ℓ ≳ 50***

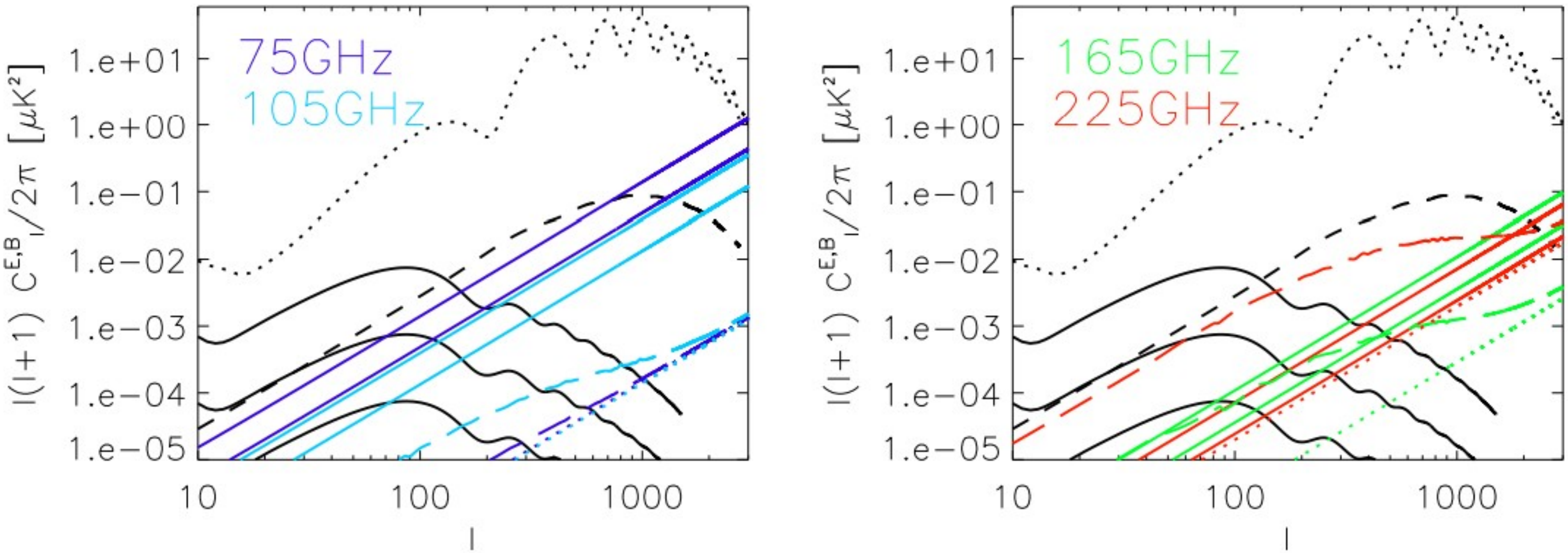


***Curto et al 2013***

# #3. What about magnetic dust (MD)?

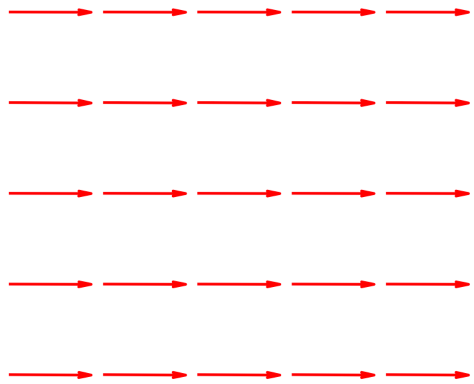

*Ferromagnetic lattice with spins aligned.*

*Thermal fluctuations will move them away, producing magnetic dipole radiation*

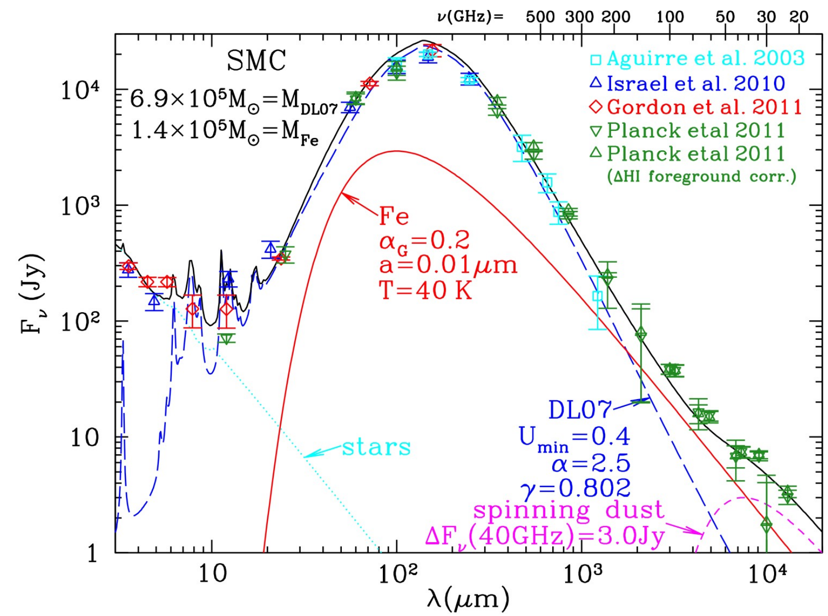


***Draine & Hensley 2013***

- **Diffuse MD not yet observed!**
- **In theory, MD might be highly polarized ~35%**
- **Spectral degeneracy at ~ 100 GHz between CMB and MD**

**→ *can be a killer for component separation***

# #4. Averaging effects

**The actual foreground SED <u>on the maps</u> differs from the real SED <u>in the sky</u> !**

***Chluba, Hill, Abitbol, 2017***

*Dust spectral indices in the sky*

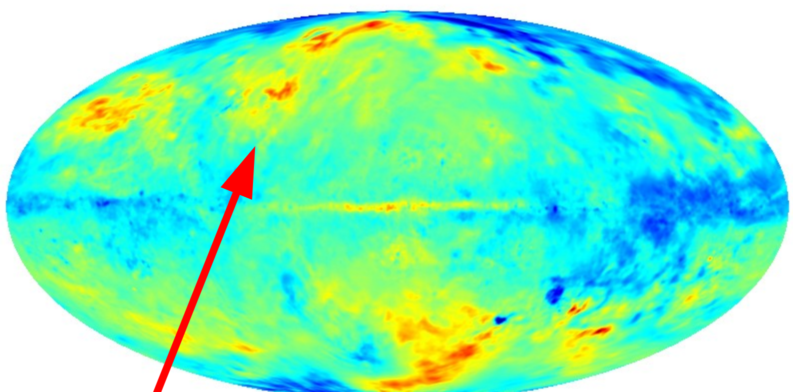

***one value $\beta_{dust}$ per line-of-sight***

*Mapping / pixelization*

***many values $\beta_{dust}$ per pixel***
***(effective SED: $\sum_i \nu^{\beta i} = \nu^{\beta + C\, Log(\nu) + \dots}$)***

**Pixelization/averaging creates spurious curvatures on the foreground SED!**

**→ Bias of $\Delta r \approx 10^{-3}$ if ignored in the parametric fitting**

***Remazeilles et al 2017,***
***for the CORE collaboration***

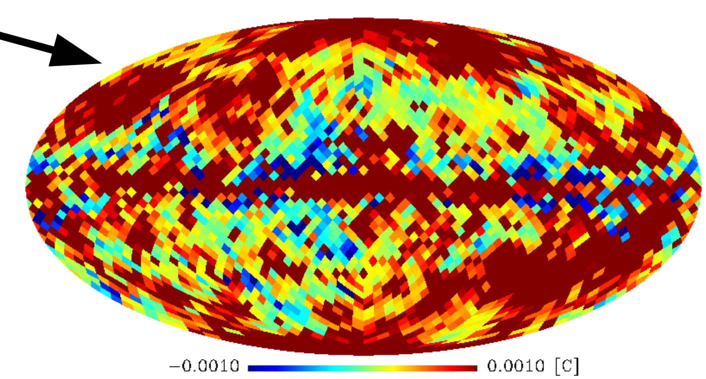

# Anisotropic μ-type distortions at $z > 10^4$

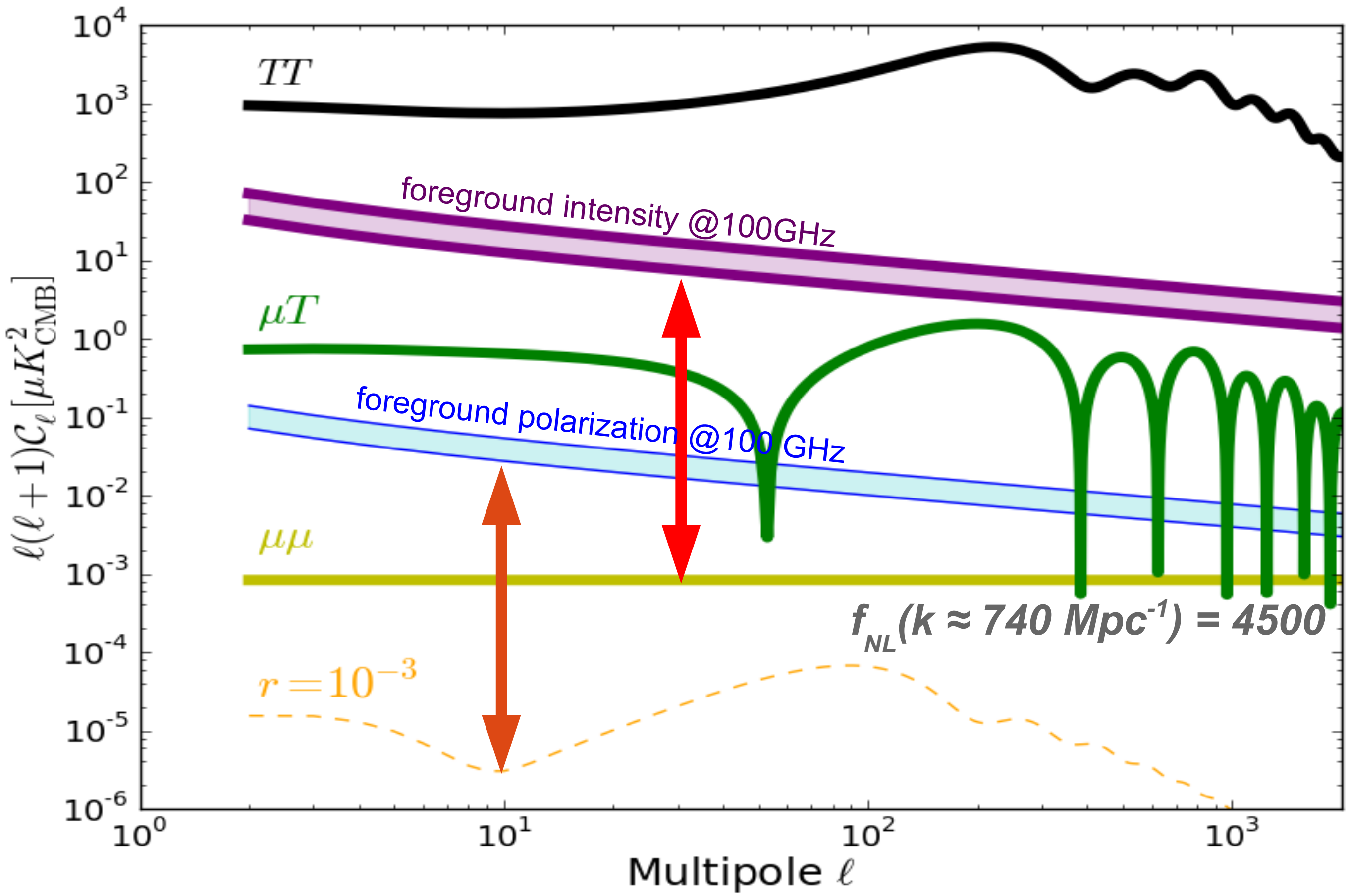


***μ-T correlation signal between CMB temperature and μ-distortion anisotropies***

***→ accessible signal, allowing to constrain $f_{NL}(k \approx 740\ \mathrm{Mpc}^{-1})$***

***→ to be definitely considered by future CMB satellites!***

***More details in Remazeilles & Chluba, MNRAS (2018): arXiv:1802.10101***